NANOINDENTATION SIZE EFFECTS IN WOOD

Joseph E. Jakes,[1] Donald S. Stone,[2] and Charles R. Frihart[1]

[1]USDA Forest Service, Forest Products Laboratory, Madison, Wisconsin U.S.A.
[2]University of Wisconsin, Madison, Wisconsin U.S.A.
jjakes@fs.fed.us

Introduction

Adhesives have been used for a hundred years in the fabrication of structural wood components such as glued laminated beams and panels, trusses, and propellers. Adhesive penetration into the wood, which can occur at both nanometer and micrometer scales, is an important factor in producing durable adhesive–wood bonds. At the micrometer scale, adhesives penetrate and fill cell lumens to provide a mechanical interlock. At the nanometer scale, some adhesives diffuse into cell walls and possibly react with polymeric components of wood, but how this diffusion affects mechanical properties of the cell wall is not clear. Studying the effects of interactions between adhesives and the nanosized composite structure of cell walls using nanoindentation can provide valuable insight towards understanding the durability of wood bonds.

Nanoindentation is a mechanical testing technique in which an indenter, typically a pyramid or sphericonical diamond probe, is pushed into a material and then withdrawn while the load and displacement of the probe are continuously recorded. The size and precise shape of the probe, along with the precision with which load and displacement can be controlled, allow the method to be used for testing volumes of material with dimensions as small as 0.1μm.

Wimmer et al. [1] were the first to prove the capability of nanoindentation to determine mechanical properties of cell walls in wood. Since their work, a number of studies around the world have employed nanoindentation to characterize wood cell walls, including Konnerth and Gindl, [2] who examined cell walls in the interphase of adhesive–wood bonds. The four adhesives used in this study were melamine-urea-formaldehyde (MUF), phenol-resorcinol-formaldehyde (PRF), polyvinylacetate (PVAc), and one-component polyurethane (PUR). The reported hardness and modulus of the cells in the MUF and PRF interphases increased as compared with reference cells outside the interphase region, while the same cell wall properties in the PUR and PVAc interphases decreased. This decrease in cell wall hardness and modulus were attributed to the PUR and PVAc adhesives' inability to penetrate the cell wall and repair the damage caused by the machining used to prepare the surface.

Wood nanoindentation studies in the literature have several features in common. First, experiments are performed on cross sections prepared on the transverse plane of cell walls. In all but one study in the literature, specimens were first embedded in Spurr's epoxy [3] to aid in microtoming and to support the cell structure during testing. This embedment may have introduced changes in properties through chemical modification. The exception was Zickler et al. [4], who embedded wood specimens in PMMA and prepared the surface by grinding and polishing. Scanning electron microscopy (SEM) images revealed that the lumens were still open, but grinding and polishing may have caused a large amount of mechanical damage on the surface.

To calculate hardness and modulus, experimenters usually employ the standard Oliver and Pharr [5] method of data analysis in which the area of the indent is calculated based on depth of the indentation and an area function, usually with no independent verification that the areas are correct. Also, almost all authors [1,2,4] specify the hardness and modulus from a specific load. This begs the question of whether or not properties depend on size of the indent, especially given that properties at the near-surface might have changed due to surface preparation technique and due to the fact that nearby features, such as cell lumens and middle lamella, might influence measured properties when indents become comparable in size to the thickness of the cell wall (see Figure 1). Typical indents on the S2 layer of the cell wall range from 0.1 μm to 2 μm across.

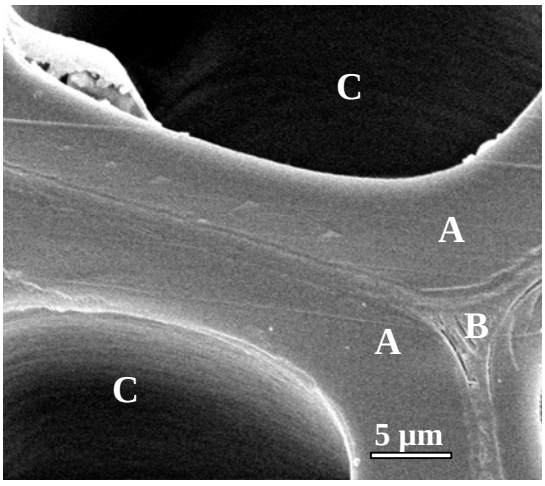

Figure 1. Scanning electron micrograph of transverse plane of S2 cell wall layer (A), middle lamella (B), and lumen (C). (SEM courtesy of Jim Beecher, FPL.)

Objectives and Scope

The purpose of this work was to test some of the assumptions underlying methods currently employed to investigate nanoindentation properties of wood. We examined whether hardness and modulus depend on load. We employed a surface preparation technique that minimizes alterations of cell wall properties. Areas were determined using both (a) Oliver-Pharr method and (b) a calibrated atomic force microscope (AFM).

Experimental Work

Specimen preparation

Nanoindentation experiments must be performed on a properly prepared surface. An ideal surface preparation technique creates a sufficiently smooth surface without altering material properties. As stated previously, others [1,2,4] have used embedments and microtoming or grinding and polishing. To limit the amount of mechanical damage on the surface and eliminate the possibility of undesired chemical modifications, we developed a surface preparation method that avoided embedment, grinding, and polishing. On a 10-mm cube of loblolly pine, we produced a gently sloping pyramid-shaped surface on the transverse plane (Figure 2). Steps were taken to ensure that the apex was positioned in the latewood. Next, a sled microtome fit with a custom-built diamond knife holder was used to cut the tip of the apex. This procedure revealed an exceptionally smooth surface of area 0.25–0.5 mm^2. Best results were achieved when the clearance angle and cutting angle were both set to approximately 5º. Figure 1 shows an SEM image of the resulting surface. We anticipated that this surface preparation technique would allow measurement of the *in situ* mechanical properties of the wood cells with fewer artifacts than possible with other surface preparation techniques.

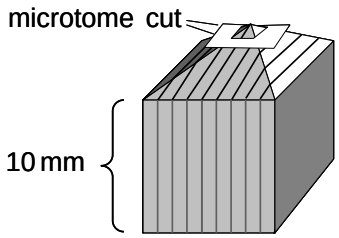

Figure 2. Specimen geometry.

Nanoindentation method

Load-controlled indents were performed on transverse planes of latewood cells in loblolly pine using a Hysitron Triboindenter equipped with a Berkovich tip. Indents consisted of a 5-s loading segment followed by a 5-s hold at maximum load and 5-s unload. Eight indents were performed in a series on one side of a cell wall consisting of 50-, 100-, 150-, 200-, 250-, 500-, 750-, and 1,000-µN indents. From the initial portion of the unloading slope, the stiffness was calculated. In nanoindentation, the Meyer hardness H is

$$H = L/A \qquad (1)$$

where L is load at the end of the 5-s hold and A is area of the indent. Likewise, we calculate the 'reduced' elastic modulus E_r from the unloading compliance C according to

$$C = \frac{\sqrt{\pi}}{2E_r}\frac{1}{\sqrt{A}} + C_m \cdot \qquad (2)$$

where C_m is machine compliance. Recent calculations on rate-sensitive materials (of which wood is one) suggest that the numerical factor $\sqrt{\pi}/2$ = 1.128 should be closer to 1.18 [7], but 1.128 is used widely in the literature so we employ it here.

Experimental data were analyzed using two methods. The first, which we call "machine analysis" because it is automatically performed by the nanoindenter software, employs the Oliver–Pharr [5] approach to calculate area as a function of depth. This method assumes that the machine compliance is the same as that measured using the fused-silica calibration standard. As we show below, the machine method introduces some artifacts. The second method employs AFM images of the indents to measure the areas directly. We also use Equation (2) along with an area-independent analysis [6] to estimate machine compliance directly from the experimental data. We refer to this second method as the "improved analysis."

Results and Discussion

Indent areas were measured from AFM images such as the ones shown in Figure 3. In this figure, the smallest and largest indents of the series are displayed. The measured areas are 0.087(6) µm^2 and 2.46(3) µm^2, respectively.

For the loads employed in this study (50–1,000 µN) and to within experimental error, we find no strong evidence that an indentation size effect is present in either H or E_r. This result is illustrated in Figure 4 for two series of indents (eight indents each) placed on the S2 layer of the cell walls. Here, the hardness and modulus remain relatively unchanged when AFM areas are used to calculate these parameters according to the improved analysis. When the machine analysis is used, the hardness and modulus appear to increase slightly at low loads. But as discussed below, these increases are artifacts.

Hardness values calculated using the improved analysis and machine analysis agree at high loads in Figure 4, but they deviate from each other at small loads. The reason for the discrepancy is that the nanoindenter has difficulty detecting the surface and therefore is not able to calculate areas accurately for low loads. For instance, for our instrument the noise in the load is about 1 µN. This corresponds to an indent approximately 50 nm across, which is over 10% of the diameter of the smallest indent in Figure 3. In other words, by the time the load can be detected there is already a sizeable indent in the material, and the depth of this indent may not be taken into account

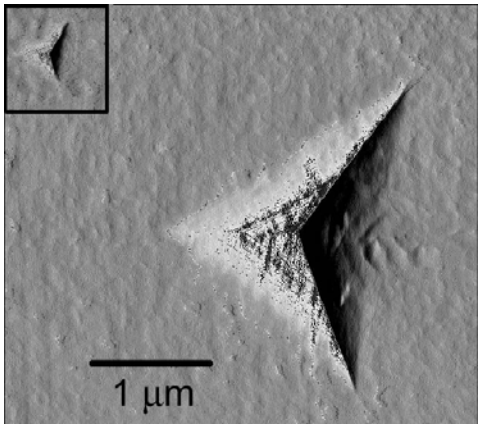

Figure 3. AFM images of the 50-µN (upper left) and 1,000-µN indents

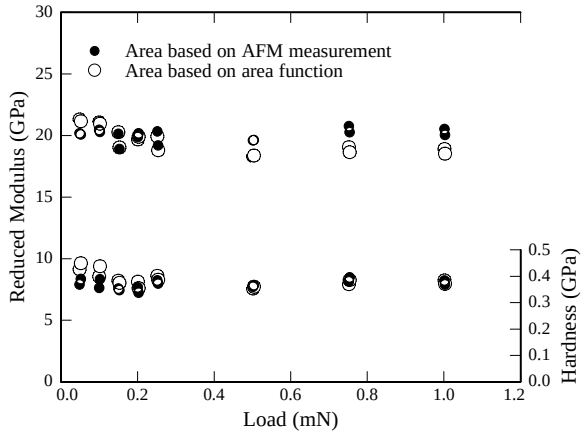

Figure 4. Hardness (H) and reduced modulus (E_r) values calculated using areas determined from AFM images and the area function.

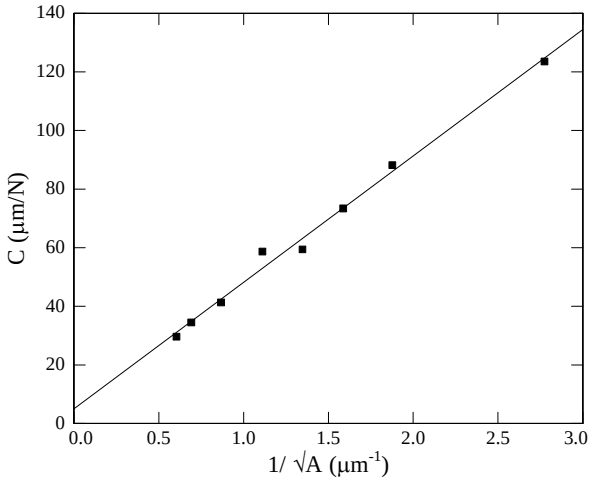

Figure 5. Plot of C vs. $1/\sqrt{A}$ using areas determined from the AFM.

properly in the contact depth used in the area function of the machine analysis. The error is more significant at low loads (50–100 µN), in which case it is better to rely on a direct measurement of area.

In Figure 4, the modulus obtained using the improved analysis is nearly flat, independent of load. The modulus based on machine analysis decreases with increasing load. Again, the discrepancy at low loads results from the indenter's inability to detect the specimen surface, which results in underestimation of area using machine analysis. At high loads, however, there is still a discrepancy between the two methods even though the areas obtained using the machine analysis are correct. In this case the discrepancy is caused by an added compliance not accounted for in the machine analysis, as explained below.

A series of indents can be analyzed using Equation (2) by plotting C vs. $1/\sqrt{A}$. According to Equation (2), the slope is inversely proportional to E_r and the intercept is the machine compliance. This is displayed in Figure 5 for one series of indents. Machine compliance from this plot is approximately 3 µm/N. In previous experiments performed on fused silica, the machine compliance was only 1 µm/N. Figure 5 suggests that an additional compliance is present in the experiment. We believe this compliance might be from flexing of the wood cell walls. Another possibility is that thermal drift is not being accounted for properly during the experiment, and that it shows up as a spurious compliance in the experimental data. We are currently investigating these two possibilities. In Figure 4, E_r calculated employing the improved analysis accounted for a machine compliance of 3 µm/N. The machine analysis utilizes a machine compliance of 1 µm/N. This difference accounts for the discrepancy between the reduced modulus values at high loads in Figure 4.

Conclusions

We have developed a method to prepare surfaces suitable for nanoindentation on the transverse plane of wood cell walls without embedment or grinding and polishing. For this sample preparation method and to within experimental error, no indentation size effect is apparent in either hardness or modulus for the S2 cell wall layer. Area measurements determined from the area function and AFM images are in agreement for the deeper indents in this experiment but deviate at shallower indents, possibly because of difficulty in detecting surface contact.

References

1. R. Wimmer, B.N. Lucas, T.Y. Tsui, and W.C. Oliver, *Wood Sci. Technol*, 1997, 31, pp 131-141.
2. J. Konnerth and W. Gindl, *Holzforschung*, 2006, 60, pp 429-433.
3. A.R. Spurr, *Ultrastructure Res.*, 1969, 26, p 311.
4. G.A. Zickler, T. Schöberl, and O. Paris, *Phil. Mag.*, 2006, 86, pp 1373-1386.
5. W.C. Oliver and G.M. Pharr, *J. Mater. Res*, 1992, 7, pp 1564-1583.
6. D.S. Stone, K.B. Yoder, and W. Sproul. *J. Vac. Soc. Technol. A*, 1991, 9(4), pp 2543-2547.
7. A.A. Elmustafa, D.S. Stone, S. Kose. Unpublished.

PROCEEDINGS

30th Annual Meeting

of

The Adhesion Society, Inc.

February 18-21, 2007
Tampa Bay, FL

Anand Jagota, Program Chair

ISSN 1086-9506